Chapter 2 Literature Review

Polymer crystallization has been a fascinating topic in the last several decades since the discovery of the chain folded lamellar crystal structure in 1957.[1] The kinetics of polymer crystallization and morphology are controlled by various factors such as molecular weight, chain flexibility, chain defects, and stereo-regularity, etc., which is different from that of small molecules. The crystallization process is also affected by experimental conditions such as temperature, pressure, nucleating agents, and stress, etc. Although great achievements in this field have been made in the last 40 years, one is still lacking a sufficient understanding of how these factors affect the crystallization kinetics. In the following, we will briefly review the morphology, the thermodynamics and the kinetic theory of polymer crystallization. Owing to the complexity of this topic, it is difficult to cover all of the important areas in this field in such a short introduction. Readers should refer to other review articles[2,3] to obtain comprehensive information about this topic.

2.1 Morphology of Semi-crystalline Polymers

It has long been known from the measurement of a variety of macroscopic properties, that while polymeric materials crystallize, they do so only partially, i.e., the bulk polymers consist of microscopic crystalline and amorphous phases. The experimental evidence includes a broad and diffuse X-ray diffraction pattern, a density that is intermediate between that of the crystal and the liquid phases, a broad melting range and a low heat of fusion, etc. In the early days of polymer morphology studies, the so-called "fringed-micelle" model was proposed in which the polymer chains thread their way through several crystallites via intermediate amorphous regions, as shown in Figure 2.1. While this model accounts for the X-ray diffraction behavior and the mechanical properties of semicrystaline polymers, it was unable to explain the optical properties of polymer spherulites and their small angle X-ray scattering patterns. The observation that polymer single crystals are very thin platelets (~ 10 nm) and that the chain axis is approximately perpendicular to the crystal basal plane led Keller to the chain-folding model.[1] In that model, a single polymer chain threads through the same crystal many

times by folding regularly on the crystal basal surfaces. Such thin platelets are called "chain-folded lamellar crystals" (see Figure 2.2). The existence of such a structure in melt-crystallized polymers was demonstrated as well,[4,5] although it is anticipated that the chain folding process is less regular in this case.

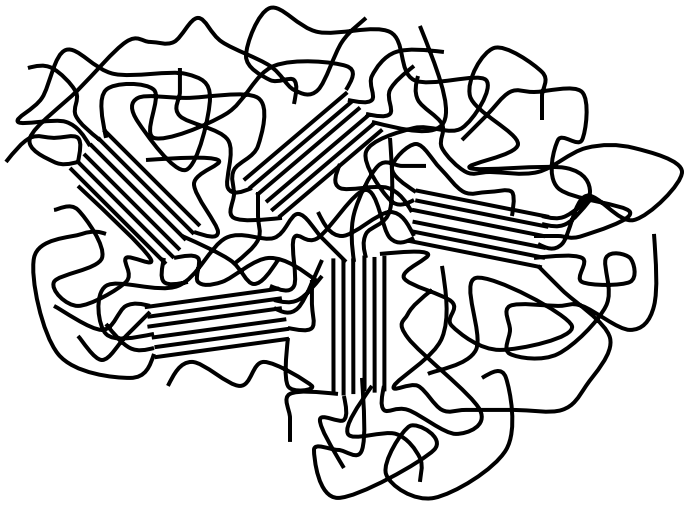

Figure 2.1 Schematic of fringed-micelle model for semi-crystalline polymers.

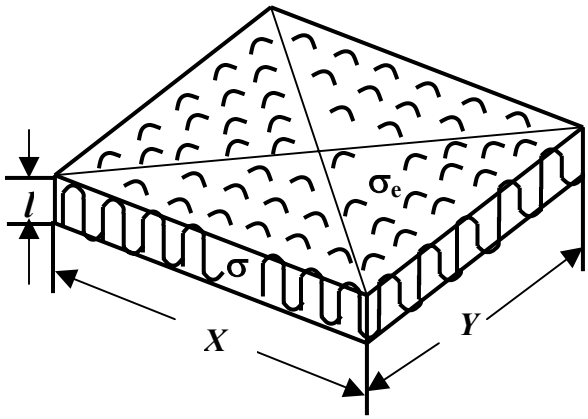

Figure 2.2 Schematic of chain-folded lamellar structure in semi-crystalline polymers with lateral dimensions *X*, *Y* and thickness *l*. σ and σ_e are the surface free energies associated with lateral and fold surfaces, respectively.

In the Introduction, we confined our discussion to melt-crystallized polymers. Although complex features have been observed for melt-crystallized polymers, many characteristics of single crystals grown from solution can also be found after

crystallization from the melt, such as chain folding, sectorization, etc. As a matter of fact, lamellar single crystals also can be grown in the melt under some specific conditions.[6]

The most commonly observed superstructures in melt-crystallized polymers are the spherulites, which consist of radiating arrays of periodic lamellar stacks. In most cases, the radius of spherulites increases linearly with time during growth under isothermal condition before the spherulites impinge on each other. The typical size of spherulites ranges from several to hundreds of microns, depending on the nucleation density. The microbeam X-ray diffraction technique has revealed that for a variety of polymers, the molecular chains are normal to the radial direction in spherulites.[8-13] Information on the molecular orientation also can be obtained from birefringence studies using polarized optical microscopy.[13] This "tangential" orientation provides important evidence for the chain-folded lamellar crystal model.

Superstructures like spherulites are often lost when short chain branches, regio or stereo defects are introduced in the chain backbone. Introduction of defects also reduces the lateral dimension and thickness of lamellar crystals and, in general, significantly inhibit the crystallization processes.

The introduction of defects into the chain backbone also decreases the frequency of adjacent reentry folding, which is the basis for the formation of regularly and tightly chain folded lamellar crystals. As a consequence, there exists a distribution of loose fold, cilia and tie chain lengths in the amorphous phase, which leads to the possibility of forming small secondary crystals in the constrained amorphous region. Other factors, such as an increase in chain length and chain rigidity, could also lead to a similar situation. The formation of secondary crystals explains the continuous increase in degree of crystallinity, which has been observed in many cases after primary crystallization. It should be noted that under specific conditions, such an increase in crystallinity after primary crystallization can also be attributed to other mechanisms such as lamellar thickening. Marand et al.[15-17] proposed a model to explain how the characteristics of polymer chains and the crystallization conditions affect the mechanism of secondary crystallization. In that model, the formation of secondary crystals occurs in a constrained environment below some critical temperature. Secondary crystals when formed at high undercooling are most likely to be of the fringed-micellar type. Above that critical

temperature, lamellar thickening is likely to be the dominant mechanism given that the α_c relaxation process, enabling chain sliding in the crystalline region, is activated.

2.2 Thermodynamics of Polymer Crystallization

Unlike small molecules, the formation of lamellar platelet-like crystals during polymer crystallization results in a large amount of specific surface area which reduces their thermodynamic stability. Two types of surface free energy, σ_e and σ have been defined, which are associated with the fold and lateral surfaces, respectively, as shown in Figure 2.2. Accordingly, the free energy of fusion for a lamellar single crystal described in Figure 2.2 can be expressed as:

$$\Delta G_f = xyl\Delta G_f^\infty - 2xy\sigma_e - 2l(x+y)\sigma \qquad (2.1)$$

Where ΔG_f^∞ is the free energy of fusion per unit volume for a perfect crystal with infinite dimension, x and y represent the dimensions of the basal crystal plane and l is the lamellar thickness defined on Figure 2.2.

For infinitely large perfect crystals, for which the effect of surface free energies is neglected, the free energy of fusion is given as:

$$\Delta G_f^\infty(T) = \Delta H_f^\infty(T) - T\Delta S_f^\infty(T) \qquad (2.2)$$

where $\Delta H_f^\infty(T)$ and $\Delta S_f^\infty(T)$ are the enthalpy and entropy changes upon fusion at temperature T. At the equilibrium melting temperature, T_m, the melt is in equilibrium with the perfect crystal of infinite size. Hence $\Delta G_f^\infty(T_m) = 0$, which gives:

$$T_m = \frac{\Delta H_f^\infty(T)}{\Delta S_f^\infty(T)} \qquad (2.3)$$

For lamellar crystals with finite dimensions, the associated melting temperature T_m' can be calculated by substituting ΔG_f^∞ with $\Delta G_f^\infty(T_m') = \Delta H_f^\infty(T_m') - T_m'\Delta S_f^\infty(T_m')$ in eq 2.1 and using eq 2.3. Assuming $x, y >> l$ and $\sigma << \sigma_e$, T_m' can be given as:

$$T_m' = T_m\left(1 - \frac{2\sigma_e}{l\Delta H_f^\infty}\right) \qquad (2.4)$$

This is the famous Gibbs-Thomson (or Gibbs-Thomson-Tammann) equation which correlates the melting temperature and the thickness of a given lamellar crystal. According to eq 2.4, the fold surface free energy σ_e and the equilibrium melting

temperature T_m can be estimated if the melting temperature can be determined experimentally as a function of lamellar thickness, given that ΔH_f^∞ is known.

It should be noted that the above derivations are based on considerations of equilibrium thermodynamics, i.e., assuming $\Delta G = 0$ for the melting process. For a kinetic process, ΔG should be less than 0. Therefore, the above equations only set some bounds for polymer crystallization process. For example, the minimum lamellar thickness l that will be stable at temperature T can be obtained from eq 2.4:

$$l_{min} = \frac{2\sigma_e T_m}{\Delta H_f^\infty \Delta T} \tag{2.5}$$

where $\Delta T = T_m - T$, which is known as the supercooling.

For polymer crystallization, it is widely accepted that the morphology and the spherulitic growth rate of semi-crystalline polymers are controlled by kinetic factors rather than by thermodynamic ones. Therefore, a kinetic theory is desired to describe the process of the crystallization. This topic is discussed next.

2.3 Kinetic Theory of Polymer Crystallization

Two main kinetic theories have been proposed including the Lauritzen-Hoffman secondary nucleation (LH) theory[17,18,19] and Sadler's rough surface or entropic theory[20,21]. Both models share the assumption of a free energy barrier. The nature of the barrier distinguishes the LH theory from rough surface theory.

The driving force for crystallization is controlled by the supercooling. To describe the driving force quantitatively, the free energy change during crystallization, ΔG_c, can be used. For a lamellar crystal showed in Figure 2.2, ΔG_c is expressed as:

$$\Delta G_c(T) = lxy\Delta G_c^\infty(T) + 2xy\sigma_e + 2l(x+y)\sigma \tag{2.6}$$

Here, $\Delta G_c^\infty(T) = \Delta H^\infty(T) - T\Delta S^\infty(T)$, $\Delta S^\infty(T) \approx \Delta S^\infty(T_m) = \Delta H^\infty(T_m)/T_m$ and $\Delta H^\infty(T) \approx \Delta H^\infty(T_m)$. In addition, the σ term in eq 1.6 can be neglected because the magnitude of the lateral dimension x, y (~10μm) is much larger than that of the lamellar thickness l (~10nm). On the basis of these assumptions, and using eq 2.5 $\Delta G_c(T)$ can be expressed as:

$$\Delta G_c(T) = lxy(2\sigma_e/l - \Delta H^\infty(T)\Delta T/T_m) = 2\sigma_e xy(1 - l/l_{min}) \tag{2.7}$$

From eq 2.7, it can be clearly seen that $\Delta G_c(T) < 0$ if $l > l_{min}$. Therefore, the larger the lamellar thickness, the larger the free energy change during crystallization, the larger the driving force.

On the other hand, in order to initiate the crystallization process, a section of chain needs to be deposited on the crystal growth front. The localization of the stem on the crystal surface is associated with a decrease in the entropy of the polymer chain. This leads to an entropic barrier that increases with crystal thickness.

The growth rate therefore is the result of an interplay between the free energy barrier and the driving force. The actual thickness of lamellar crystals corresponds to the thickness of crystals that have the largest growth rate under given experimental conditions. It should be noted that both the free energy barrier and the driving force are undercooling dependent. Besides undercooling, other factors such as the chain length and the concentration of defects on the chain backbone also have a significant influence on the growth rate and the final morphology.

2.3.1 Lauritzen-Hoffman (LH) Surface Nucleation Theory

The experimental results that the growth rate is proportional to $\exp(-1/\Delta T)$ and the formation of facetted single crystals in solution strongly suggest that polymer crystallization is nucleation controlled. On this basis, a surface nucleation theory was proposed by Lauritzen and Hoffman[17,22]. The LH model quantitatively describes how fast the growth front advances under given crystallization conditions. In this model, the lamellar crystal growth front, which is actually the lateral surface of a lamellar crystal, is thought to be smooth. In the initial stage, as shown in Figure 2.3, a molecular stem attaches itself to this smooth crystal substrate, leading to an activated state without crystallographic registration. This process, which is called surface nucleation or secondary nucleation, generates two new lateral surfaces, leading to an increase of the overall free energy ($\Delta\phi_1 = 2b_0\sigma l$) as shown in Figure 2.4. Here, b_0 is the thickness of the layer. In the LH theory, this first step is associated with the largest energy barrier and is therefore considered as the rate-determining step. The magnitude of this barrier increases with the lamellar thickness (l). In the second step, the segments become crystallographically registered and a certain free energy ($\Delta\phi_2 = -a_0b_0l\Delta G_f$) is released,

where a_0 is the width of the stem. In the following steps, subsequent stems fold back and are deposited adjacent to the attached stems to further lower the overall free energy until reaching a negative global free energy change. The free energy change associated with this sequential folding process is $\Delta\phi_\nu = (n\text{-}1)a_0b_0(2\sigma_e - l\Delta G_f)$.

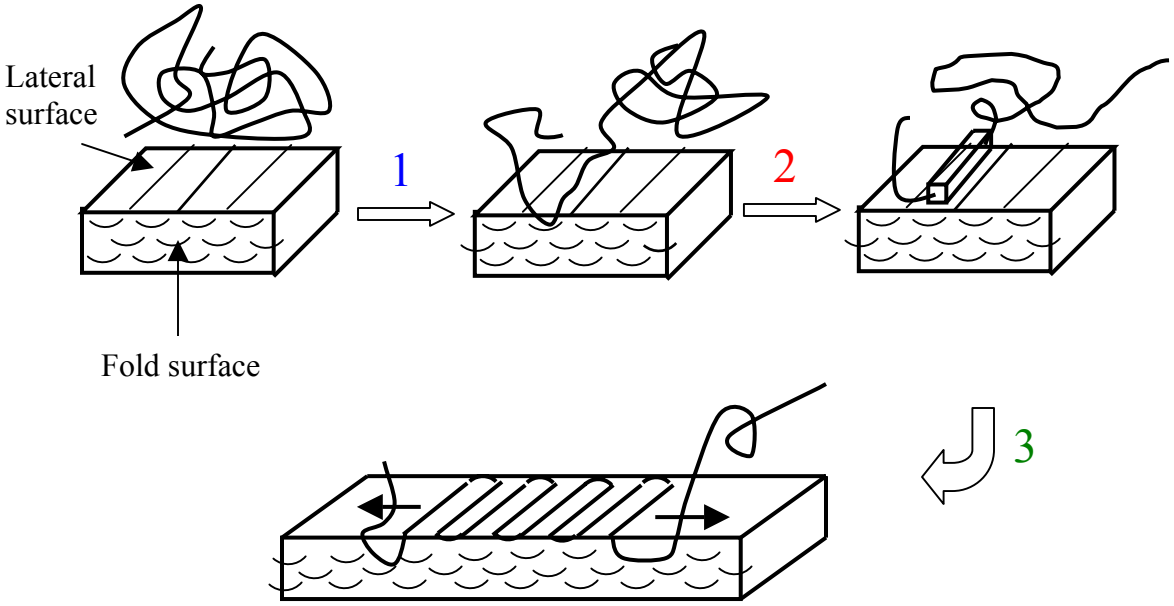

Figure 2.3 Schematic of the surface nucleation process on the crystal growth front (see the text for the description)

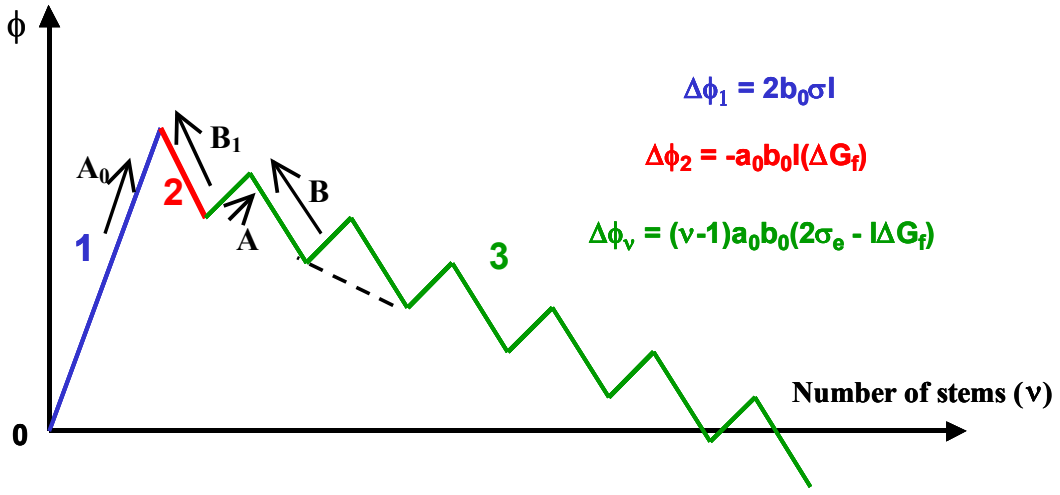

Figure 2.4 Free energy evolution of formation of a chain-folded nucleus. (See the text for the description.)

With these free energy barriers, the rate constant for each step can be obtained using an Arrhenius expression:

$$A_0 = \beta \exp(\frac{-2b_0\sigma l}{kT}) \tag{2.8}$$

$$B_1 = B = \beta \exp(\frac{-a_0 b_0 l(\Delta G)}{kT}) \tag{2.9}$$

$$A = \beta \exp(\frac{-2a_0 b_0 \sigma_e}{kT}) \tag{2.10}$$

where A_0 is the rate constant for attainment of the activated state, B and B_1 are those for removing an attached stem back to the melt state (here B_1 is for removing the first stem), A is that for the forward reaction for the deposition of each stem when $v \geq 2$, β is a factor that accounts for retardation due to transport of chain segments to or from the growth front and, ΔG is the free energy of fusion at the crystallization temperature.

With these rate equations, the flux of stems of length l over the nucleation barrier can be determined in the general case[23] as:

$$S(l) = N_0 A_0[(A - B)/(A - B + B_1)] = N_0 A_0(1 - B/A) \tag{2.11}$$

Where N_0 is the number of reacting species which can be defined as $N_0 = C_0 n_L$, where C_0 is the configurational path degeneracy and n_L is the number of stems with width a_0 comprising the substrate length L. The net flux across the nucleation barrier therefore can be calculated:

$$S_T = \frac{1}{l_u}\int_{2\sigma_e/\Delta G}^{\infty} S(l)dl \tag{2.12}$$

where l_u is the monomer length. Using the definition of surface nucleation rate i:

$$i \equiv S_T/L = S_T/\, n_L a_0 \tag{2.13}$$

one obtains:

$$i = \frac{C_0\beta}{a_0 l_u}\left(\frac{kT}{2b_0\sigma} - \frac{kT}{2b_0\sigma + a_0 b_0 \Delta G}\right)\exp\left(\frac{-4b_0\sigma\sigma_e}{\Delta G kT}\right) \tag{2.14a}$$

In the case of PE, $a_0 b_0 \Delta G$ is much less than $2b_0\sigma$. Therefore eq 2.14a can be simplified to be:

$$i = \frac{C_0 \beta}{a_0 l_u}\left(\frac{kT\Delta G}{4b_0 l_u \sigma^2}\right) exp\left(\frac{-4b_0 \sigma \sigma_e}{\Delta G kT}\right) \tag{2.14b}$$

Similarly, the initial lamellar thickness (l) can be obtained by performing a statistical mechanical average with the flux being the weight factor:

$$< l >= l_g^* = \frac{\frac{1}{l_u}\int_{2\sigma_e/\Delta G}^{\infty} lS(l)dl}{\frac{1}{l_u}\int_{2\sigma_e/\Delta G}^{\infty} S(l)dl} \tag{2.15}$$

This yields:

$$\begin{aligned} l_g^* &= \frac{2\sigma_e}{\Delta G} + \frac{kT}{2b_0\sigma}\left(\frac{\Delta G + 4\sigma/a_0}{\Delta G + 2\sigma/a_0}\right) \\ &= \frac{2\sigma_e}{\Delta G} + \delta \\ &= \frac{2\sigma_e T_m}{\Delta h_f \Delta T} + \delta \end{aligned} \tag{2.16}$$

where $\delta = \frac{kT}{2b_0\sigma}\left(\frac{\Delta G + 4\sigma/a_0}{\Delta G + 2\sigma/a_0}\right)$. Under low and moderate undercooling, δ can be approximated as:

$$\delta \cong \frac{kT}{b_0\sigma} \tag{2.17}$$

Hence the LH theory predicts (eq 2.16) that the initial lamellar thickness is a linear function of $1/\Delta T$, which has been observed experimentally.

The substrate completion rate, g, is defined to be:

$$g \equiv a_0(A - B) \tag{2.18}$$

Using eqs 2.9 and 2.10, g is determined to be:

$$g = a_0 \beta\, exp\left(\frac{-2a_0 b_0 \sigma_e}{kT}\right)\left[1 - exp\left(\frac{-a_0 b_0 \delta \Delta G}{kT}\right)\right] \tag{2.19}$$

At low-to-moderate undercooling, the second exponential term in eq 2.19 can be expanded and using eq 2.17 and $\Delta G = \Delta H_f \Delta T / T_m$, g can be approximated to be:

$$g = a_0 \beta \left(\frac{a_0 \Delta H_f \Delta T}{\sigma T_m} \right) exp\left(- \frac{2 a_0 b_0 \sigma_e}{kT} \right) \tag{2.20}$$

It should be noted that, as a coarse model, LH theory treats the attachment of the stems onto the substrate as a one-step process and ignores the entropic character of the nucleation event and subsequent spreading of the stems in the early development of this theory. Recently, the segmental nature and entropic origin of the initial surface nucleation process have been considered by Hoffman et al.[24] They correlated the lateral surface free energy σ with the characteristic ratio C_∞ and attributed the free energy barrier of the surface nucleation to an entropic origin. However, they still deny an entropic character to the substrate completion process. In the LH formalism, since there is no new lateral surface generated during substrate completion, the only free energy barrier during this process is associated with folding (i.e., creation of the fold surface of free energy of σ_e). In addition, this free energy contribution from σ_e is not related to the lamellar thickness, therefore according to eq 2.20, the substrate completion process weakly depends on the undercooling compared with the surface nucleation process which has an exponential dependence of undercooling.

In LH theory, the existence of three regimes can be predicted according to the competition between *i* and *g* as shown on Figure 2.5.

At high temperature, the surface nucleation is very slow which controls the overall growth rate *G*. This temperature range is defined as regime I in which *G* can be expressed as:

$$G_I = b_0 i L \tag{2.21}$$

where b_0 is the thickness of the layer and *L* the substrate length. To ensure the constant growth rate during isothermal crystallization, which is normally observed during growth rate measurements for spherulites from melts and single crystals from solution, a constant *L* is needed. A problem was raised when investigators dealt with the single crystal case in which L is identified with the length of the edge of the single crystal. Since the length of edge will increase with the growth of the crystals, increased growth rate is expected which contradicts the experimental observations. To avoid this, a concept "persistence length" was suggested[25,26] for *L*, which is smaller than the crystal edge. The persistence length stays constant during growth, therefore giving a linear growth behavior.

In the intermediate temperature range, which is defined as regime II, the growth rate is controlled by both *i* and *g* and can be calculated as:

$$G_{II} = b_0(2ig)^{1/2} \qquad (2.22)$$

It should be noted that the substrate completion rate *g* in the LH model is weakly dependent on temperature. Therefore the regime transition behavior is due to the strong dependence of *i* on the temperature. Comparison of eqs 2.21 and 2.22 will lead to a quantitative description of regime I and II as follows. If $iL^2/2$ is much larger than g, regime II behavior can be observed. Regime I is expected when $iL^2/2$ is much smaller than g. This situation is showed on Figure 2.6 using the data of polyethylene fraction (M_w = 30 kg/mol) by Armistead and Hoffman[27]. The regime I//II transition occurs around the crossing point of the curves of $iL^2/2$ and g as shown on Figure 2.6(a).

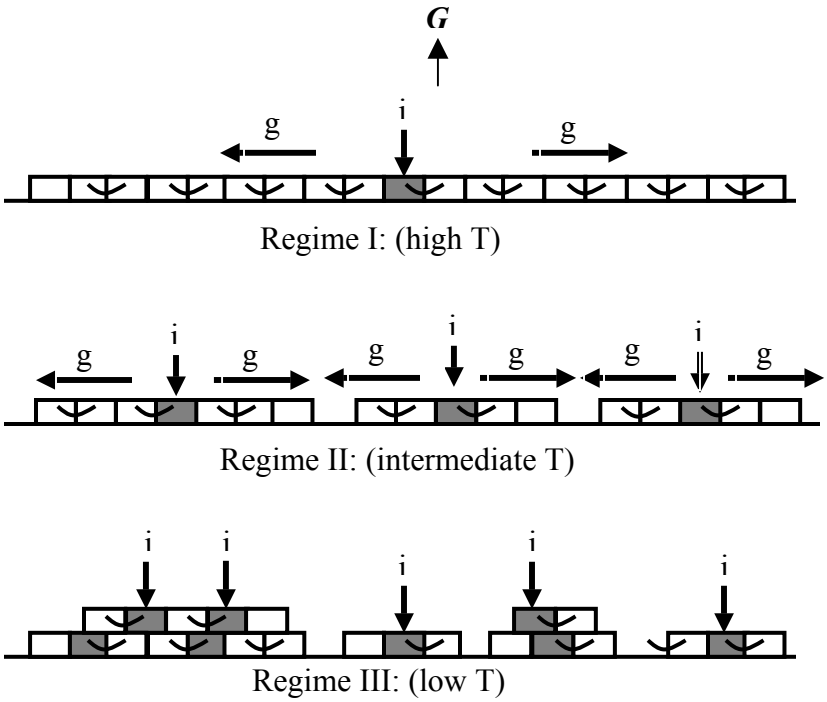

Figure 2.5 Schematic of the crystal growth in Regime I, II and III according to the LH theory.

To describe the distinction between regime I and II quantitatively, a dimensionless quantity $Z = iL^2/4g$ was proposed by Lauritzen. Regime I behavior is expected if $Z \leq 0.01$, while regime II is reached when $Z \geq 1$. The range between $Z = 0.01$ and 1 defines the transition region from regime I to II as indicated on Figure 2.6(b), which is around 2 to 3 K in the case of polyethylene. However, the experimentally

observed regime I/II transition is quite sharp (transition range is within 1 K), which is not consistent with the prediction by the *Z*-test, therefore casting some doubts on the physical origin of regime I/II transition.

When the temperature is further lowered, the nucleation rate would become extremely large and there is not much space for nuclei to spread before they meet. In that case, the growth rate will be determined by the nucleation rate again as in regime I. This temperature range is defined as regime III. Similar to regime I, the growth rate in regime III also can be expressed as:

$$G_{III} = b_0 i L' \tag{2.23}$$

Here L' is the distance between niches and is only 1.5-2a_0, where a_0 is the width of stem.

An important parameter that can be used to differentiate these three regimes is the mean number of stems with width a_0 between two neighboring nucleation events, N_k. In regime I, the value of N_k should be close to the number of stems with width a_0 comprising the regime I substrate length L. Using the measured regime I/II transition temperature, the N_k at regime I/II transition has been calculated to be about 190 for polyethylene, which seems a reasonable value. In regime II, the N_k can be calculated as $(1/a_0)(2g/i)^{1/2}$. Therefore N_k should decrease with increasing undercooling in this regime. When the temperature approaches the junction of regime II and III, the value of N_k should reach 1.5 to 2. The theoretical values of N_k at $T_{I/II}$ and $T_{II/III}$ can be used as criteria to find the position of regime I/II and II/III transition. The obtained values of $T_{I/II}$ and $T_{II/III}$ seem consistent with the observed ones.[27] Figure 2.7 shows the value of N_k as a function of temperature in regime I, II, and III for the polyethylene fraction with M_w = 30 kg/mol.

With the expressions for i and g, the overall growth rate (G), can be determined:[19]

$$G = G_j^0 exp(-\frac{U^*}{R(T_x - T_\infty)}) exp(-\frac{K_{gj}}{T_x \Delta T}) \tag{2.24}$$

$$G = G_j^0 exp(-\frac{Q_d^*}{RT_x}) exp(-\frac{K_{gj}}{T_x \Delta T}) \tag{2.25}$$

a

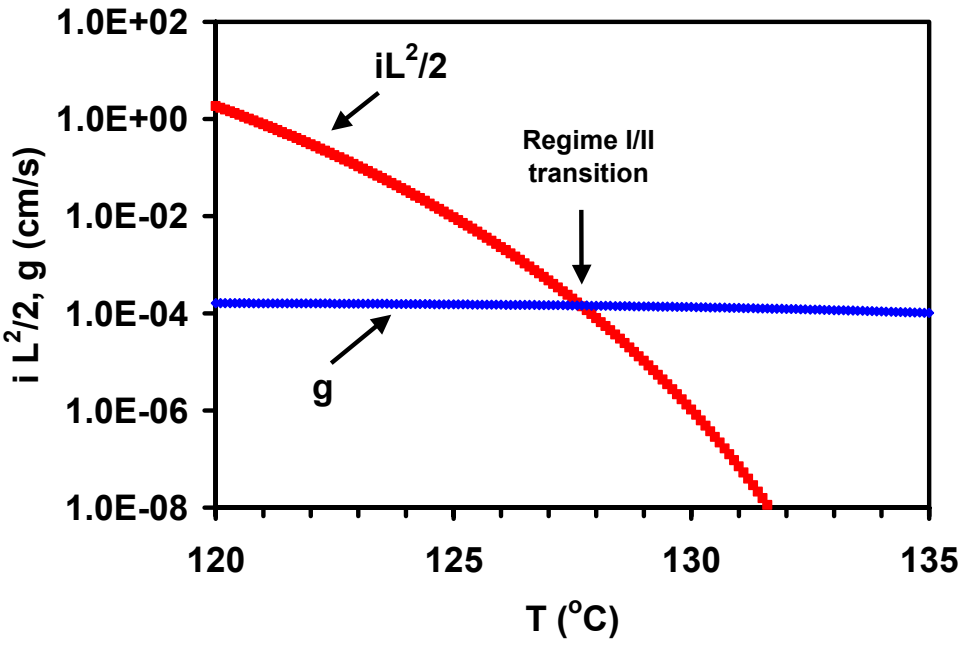

b

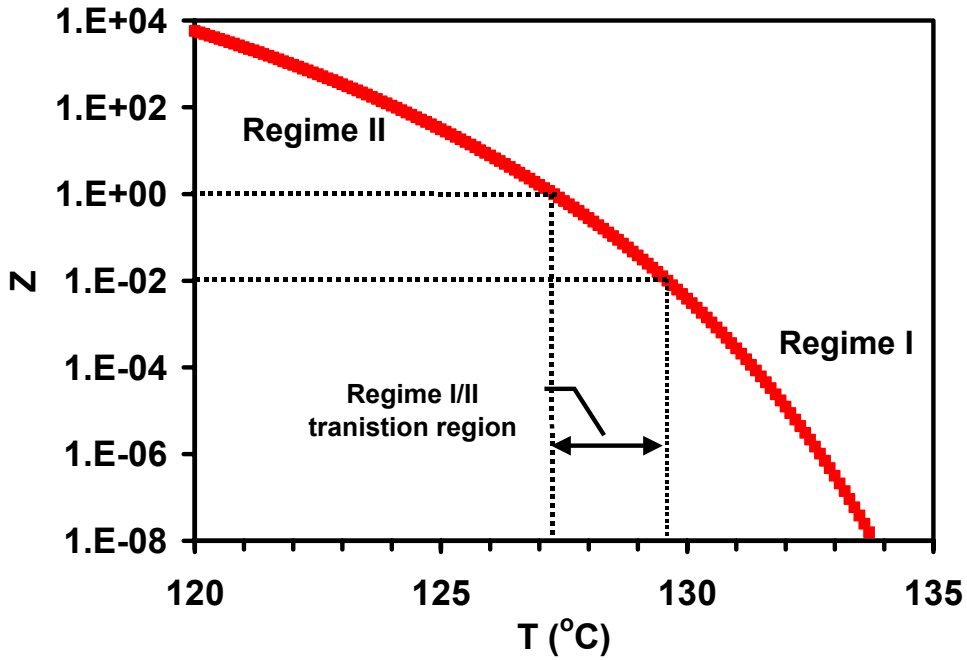

Figure 2.6 (a) The comparison between $iL^2/2$ and g. The crossing point defines the position of regime I/II transition. The data are adopted from Armistead and Hoffman for a polyethylene fraction with M_w = 30 kg/mol.[27] (b) The Z-test for the same data in (a). The range of Z from 0.01 to 1 defines the regime I/II transition range.

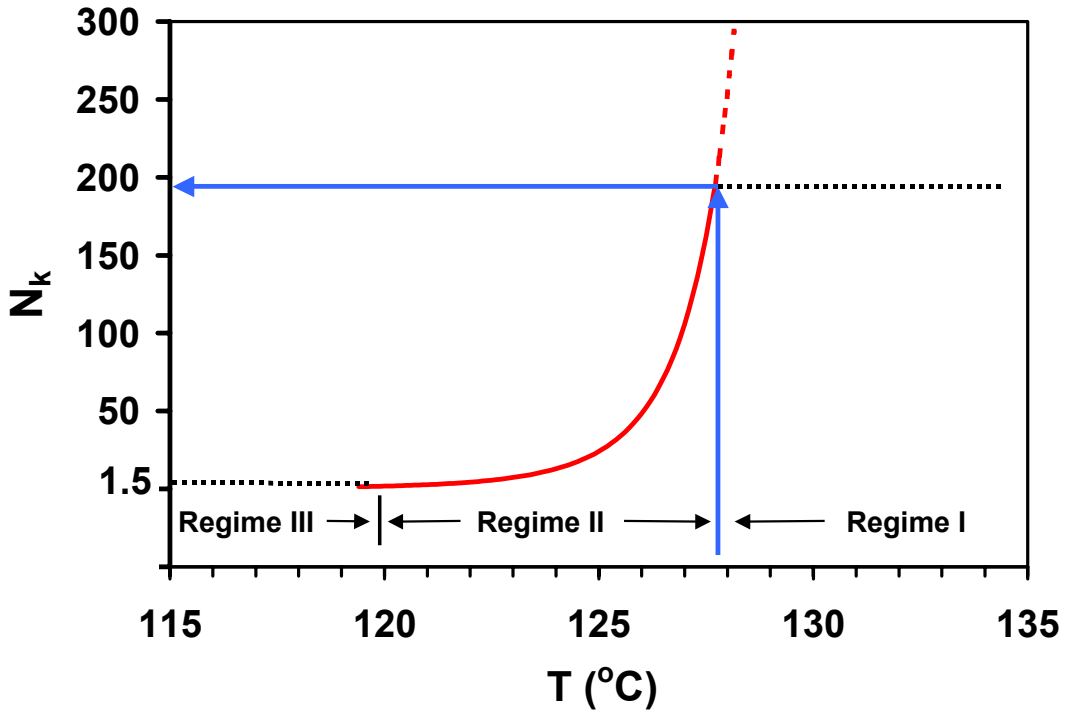

Figure 2.7 Number of stems with width a_0 between two neighboring nucleation events as a function of temperature in three regimes. The data are adopted from Armistead and Hoffman[27] for a polyethylene fraction with M_w = 30 kg/mol.

Eq 2.24 adopts the form of Vogel-Fulcher-Tamman-Hesse (VFTH) equation that describes the nonlinear behavior in the temperature region close to T_g using parameters U^* and T_∞, while eq 2.25 takes the Arrhenius form using parameters Q_d^*, the activation energy for the segmental transport. It has been suggested[19] that the eq 2.24 should be used when the temperature is below T_g + 100 K and both forms can be applied when the temperature is higher than T_g + 100 K. In eq 2.24, a universal value 6270 J/mol was suggested for U^* and T_∞ is usually taken as T_g – 30 K. In both equations, the third term on the right side controls the nucleation rate and depends on the undercooling ($\Delta T = T_m - T_x$). The parameter K_{gj} is the secondary nucleation constant and has the following expression:

$$K_{gj} = \frac{jb_0\sigma\sigma_e T_m}{\Delta H_f k} \qquad (2.26)$$

where k is the Boltzmann's constant. The parameter j varies with regime: j = 4 in regime I and III and j = 2 in regime II. Therefore it can be predicted that $K_{g(I)} = K_{g(III)} = 2K_{g(II)}$,

which is an important criterion for the LH theory. The quantitative relationship between K_g values in the three regimes is also implied by eqs 2.21 - 2.23. The K_g values can be determined by plotting $\ln G + U^*/R(T_x - T_\infty)$ against $1/T_x\Delta T$, making the so called LH plot. The product of surface free energy $\sigma\sigma_e$ can be calculated from K_g. Combined with other methods to determine the lateral surface free energy σ, σ_e can be obtained. Therefore, through comparing this value of σ_e with those inferred from other approaches, LH theory can be further tested.

Various polymers were found to exhibit regime transition behavior through spherulitic growth rate measurements or/and overall kinetics study. Three regimes have been identified in polyethylene fractions,[27] cis-1,4-polyisoprene,[28] isotactic poly(1-butene),[29] poly(3,3-dimethylthietane)[30,31], and poly(L-lactic acid).[32,33] Regime I/II transition has been reported for poly(ethylene oxide),[34-36] and poly(1,3-dioxolane).[37] Examples reported for regime II/III transition include isotactic polypropylene,[39-42] syndiotactic polypropylene,[42] poly(oxymethylene),[43] poly(p-phenylene sulphide),[44] poly(3-hydroxybutyrate),[45] poly(pivalolactone),[46] poly(trimethylene terephthalate)[47], and poly(ethylene succinate).[48]

Besides the breaks in the crystallization temperature dependence of spherulitic growth rates, morphological transitions were also found in some polymers. Distinct morphological differences in three regimes of PE were observed by polarized microscopy.[18,19,27] Bassett et al.[49] reported that ridged sheets are dominant in regime I while S-shaped lamellar sheets are usually dominant in regime II. Phillips and Vatansever[28] observed an obvious change in the number of branches per lamella in different regimes for cis-polyisoprene. Except for these polymer systems, a firm evidence for significant morphological transitions accompanying regime transitions is still absent. In most cases, the morphological changes observed optically are gradual and accompanied by the loss of birefringence with decreasing undercooling.

2.3.2 Rough Surface Theory

Although the LH theory successfully predicts the undercooling dependence of growth rate, the regime transition behavior and the undercooling dependence of the lamellar thickness, there are still some problems associated with this theory. First, the LH

theory neglects the fluctuations in lamellar thickness. In the LH theory, the stems deposited on the substrate have a fixed length and the substrate completion step is very fast and weakly dependent of the undercooling. Here, the LH theory only considers the free energy difference between the states before and after deposition. However, it has been suggested that the stem length might undergo some random fluctuations during the substrate completion process, which would lead to a rugged free energy landscape. It is possible that the deposition will be stuck in some local free energy minimum and some activation energy needs to be overcome to resume the deposition. This activation energy is likely to be larger than the free energy change contributed by the folding process, which constitutes the free energy barrier in the propagation process in the LH theory. This situation is similar to the entropy frustration described by Muthukumar[50] in the case of patterned adsorption and the glass transition behavior of supercooled liquid for which the thermodynamic free energy minimum is always hard to reach. This leads to a strong entropic barrier in the process of substrate completion, which depends on the lamellar thickness. Therefore, a significant undercooling dependence should be expected for the substrate completion rate, which is in contradicted with the LH theory, where g is weakly dependent on undercooling.

Sadler and Gilmer[20,21,50-52] proposed a rough surface model that focuses on this entropic barrier in the propagation of stems on the substrate. As they claimed, the surface nucleation (the deposition of first stem on growth front) has little effect on the growth rate based on the assumption of roughness of the growth front. In their model, the deposition of stem is visualized as a process of zippering down of segments in which the addition and removal of segment are reversible. In contrast with the LH theory, the segments can undergo folding at anytime during the zippering down process leading to a rough fold surface and a possible tapered shape. Therefore, some short stems with length less than l^* (the minimum stable stem length) need to be removed to resume the further propagation. This generates some byroads for growth that can be considered as entropic barriers mentioned above. Obviously, with increasing l^*, which means with increasing the crystallization temperature, more byroads will be generated, which greatly increases the entropic barrier thus decreases the growth rate. The calculations based on the rate

equation and Monte Carlo simulation by Sadler and Gilmer[21,52-54], Goldbeck-Wood et al.[54] showed on undercooling dependence of lamellar thickness and growth rate, which is qualitatively consistent with experimental results. The rate-equation model also successfully explains the self-poisoning effect exhibited by alkane crystallization at transition from extended-chain crystals to once-folded chain crystals.[56-59]

Recently, Doye, Frenkel[59,60] and Toda[61] tried to reconcile the surface nucleation model and the rough surface model by emphasizing both surface nucleation and entropic barrier in the propagation process. In the picture provided by Doye and Frenkel,[59,60] the nucleus formed on the substrate consists of several stems in contrast to the one stem assumption in the LH theory. In addition, the thickness of the layer formed last is not determined by the thickness of the nucleus but results from a convergence process that is related to the entropic barrier for the deposition of segments. Applying similar idea, Toda studied the undercooling dependence of the growth rate using rate equations and Monte Carlo simulations.[61] His calculations indicate that the substrate completion rate is an exponential function of the lamellar thickness (i.e., the inverse of undercooling). A dramatic change in substrate completion rate with undercooling has been observed in some specific cases, like the growth on the (200) face in polyethylene single crystal. It is expected that the kinetic substrate length ($L_k = (g/2i)^{1/2}$), which is the distance between two neighboring nucleus, will become weakly dependent on undercooling and the regime I/II transition may vanish. Point and Colet have suggested this before. If this is true, an alternative explanation for the slope change in LH plots is needed. This will be discussed further in this work.

One of arguments about the validity of surface nucleation model and rate-equation model focuses on the explanation of curved edge crystals observed at high temperature for polyethylene. It was found that (200) sectors in PE single crystals exhibit curved edges.[62,63] Sadler et al. questioned the LH theory on this issue because this model assumes a flat growth front. To "save" the LH theory, Miller and Hoffman[64] proposed a mechanism that correlates the curved edge with the lattice strain which results from the mutual repulsion of chain folds. A parameter σ_s was proposed to characterize the internal lattice strain. With the correct σ_s, the aspect ratio and curvature can be predicted as a

function of crystallization temperature. However, this model may not be fully satisfactory as the curved edge were also found in the extended-chain single crystals of polyethylene where the chain folding is absent.

2.4 Copolymer Crystallization Theory

The crystallization of copolymers exhibits remarkably different behavior compared to that of linear homopolymers due to the introduction of chemically different co-units into the chain backbone. As a result of the different possible arrangements of co-units, copolymers can be classified as random, block or alternating copolymers. The present review is aiming at giving a brief introduction to the crystallization and melting behavior of random copolymers with special emphasis on ethylene random copolymers.

A copolymer is considered as having two types of units: crystallizable units and non-crystallizable units. We designate the former as A unit and the later as B unit. A thermodynamic model based on phase equilibrium concepts was developed by Flory.[65] According to this theory, a sequence of A units of different lengths exhibit different ability to crystallize. Only those sequences with length exceeding some critical value ζ can be incorporated into the crystalline phase at a given temperature, while shorter sequences will remain in the amorphous region. ζ is a function of crystallization temperature and increases with increasing temperature. In Flory's model, it is assumed that the non-crystallizable units B are excluded from the crystallites composed of A units. In the case of ethylene copolymers, the experimental evidence supporting this assumption was obtained using solid state ^{13}C NMR[65-73] and the technique of selective oxidation.[75] It was concluded that side-groups larger than methyl are generally excluded from the polyethylene lattice and that their concentration in the lattice can be neglected. However, small side-groups such as CH_3, Cl and OH may enter the crystal lattice on an equilibrium basis. For copolymers made with these latter counits, Flory's equilibrium theory will not be relevant.

Based on these assumptions, a relationship between the melting temperature and the sequence distribution of unit A was established by Flory:[65]

$$\frac{1}{T_m} - \frac{1}{T_m^0} = -\left(\frac{R}{\Delta H_u}\right) ln(p) \qquad (2.27)$$

Where T_m is the melting temperature of the copolymer, T_m^0 is the equilibrium melting temperature of the corresponding homopolymer (in the case of ethylene copolymers, this is polyethylene), R is the gas constant, ΔH_u is the heat of fusion per repeat unit of the homopolymer, p is the sequence propagation probability, which is the probability that a unit A is succeeded by another such unit. According to eq 2.27, T_m only depends on the sequence propagation probability (p) and is independent of the chemical nature of the co-units. Flory's model therefore predicts that a universal curve should be obtained for T_m versus p for a series of random ethylene copolymers with different comonomers. It should be noted that the experimental melting temperature is determined kinetically therefore is much smaller than the one predicted by eq 2.27. However, a universal curve for melting temperature as a function of comonomer content can still be observed in a number of experiments.[14,75,76,77] The melting temperature, as a very sensitive function of p, can be reduced by as much as 25 K through introduction of only 2 mol% branches in a linear polyethylene.[75] Moreover, if the comonomer sequence distribution is not truly random the $T_m \sim p$ plot will deviate from the universal curve predicted for the random copolymers. This was observed in several cases[78-81] and can be used to evaluate whether a given copolymer is truly a random copolymer.

The degree of crystallinity of copolymers, like the melting temperature, depends on the co-unit content and is independent of the chemical nature of the comonomer. A universal curve can also be obtained for the degree of crystallinity as a function of co-unit content.[14] However, the degree of crystallinity is not significantly affected by a small change in the sequence distribution (p) especially at low temperature.[75] After all, the degree of crystallinity has contributions from all crystallites of various types and sizes formed during crystallization. The ultimate melting temperature, on the other hand, reflects the thermodynamic stability of the most stable crystallites in the material, and is strongly affected by the sequence distribution.

Flory's thermodynamic theory provides a framework for the present work and predicts a number of trends for the evolution of the melting temperature and degree of crystallinity with sequence distribution. However, similar to linear homopolymers, the morphology of copolymers, associated melting temperature and degree of crystallinity are controlled by kinetic rather than by thermodynamic factors. Indeed, the observed

melting temperatures are much lower than those predicted by eq 2.27, which can only be achieved under equilibrium conditions.

To account for the kinetic nature of the processes involved, Sanchez and Eby[82] proposed a model based on the assumption that the comonomer can be incorporated into the crystalline region, and the extent of inclusion depends on the crystallization temperature employed. According to this model, fast kinetics results in high extent of inclusion. The depression of the melting temperature is explained by the excess enthalpy caused by the introduction of the co-units into the crystalline phase, not by an entropic effect as in Flory's theory. However, as stated above, the experimental results do not support the inclusion model. Only copolymers having a small side-group such as a methyl group can be described by the Sanchez-Eby model.

2.5 Reference

(1) Keller, A. *Phil. Mag.* **1957**, *2*, 1171.

(2) Armitstead K.; Goldbeck-Wood, G. *Advances in Polymer Science* **1992**, *100*, 219.

(3) Keller, A.; Goldbeck-Wood, G. *Comprehensive Polymer Science, 2nd Supplement* (Ed. Aggarual, S.; Russo, S) Elsevier, Oxford 1996.

(4) Palmer R. P.; Cabbold, A. *Makromol. Chem.* **1964**, *74*, 174.

(5) Keller, A.; Sawada, S. *Makromol. Chem*. **1965**, *74*, 190.

(6) Toda, A *Colloid Polym. Sci.* **1992**, *270*, 667.

(7) Point, J. J. *Bull. Acad. Roy. Belg*. **1955**, *41*, 982.

(8) Keller, A. *J. Polym. Sci*. **1955**, *17*, 351.

(9) Fujiwara, Y. *J. Appl. Polym. Sci*. **1960**, *4*, 10.

(10) Mann, J.; Roldan-Gonzalez, L. *J. Poly. Sci*. *A-2* **1966**, *4*, 243.

(11) Magill, J. H. *J. Polym. Sci.* **1962**, *60*, 1.

(12) Baltá Calleja, F. J.; Hay, I. L.; Keller, A. *Kolloid Z. Z. Polymere* **1966**, *209*, 128.

(13) Bunn, C. W.; Alcock, T. C. *Trans. Faraday Soc*. **1945**, *41*, 317.

(14) Alizadeh, A.; Richardson, L.; Xu, J. ; McCartney, S.; Marand, H.; Cheung, Y. W.; Chum, S. *Macromolecules* **1999**, *32*, 6221.

(15) Marand, H.; Alizadeh, A.; Farmer, R.; Desai, R.; Velikov, V. *Macromolecules* **2000**, *33*, 3392.

(16) Alizadeh, A.; Sohn, S.; Quinn, J.; Marand, H.; Shank, L. C.; Iler, H. D. *Macromolecules* **2001,** *34*, 4066.

(17) Lauritzen, J. I. Jr.; Hoffman, J. D. *J. Res. Natl. Bur. Stand., Sect. A,* **1961**, *64*, 73.

(18) Hoffman, J. D; Frolen, L. J.; Ross, G. S.; Lauritzen, J. I. Jr. *J. Res. Natl. Bur. Stand., Sect. A,* **1975**, *79*, 671.

(19) Hoffman, J. D; Miller, R. L. *Polymer* **1997**, *38*, 3151.

(20) Sadler, D. M. *Polymer* **1983**, *24*, 1401.

(21) Sadler, D. M.; Gilmer, G. H. *Polymer* **1984**, *25*, 1446.

(22) Hoffman, J. D.; Lauritzen, J. I. Jr. *J. Res. Natl. Bur. Stand.,* Sect. A, **1961**, *297*.

(23) Hoffman, J. D.; Davis, G. T.; Lauritzen Jr., J. I. In *Treatise on Solid State Chemistry* (N. B. Hannay, ed.), *Vol 3*, Plenum Press, NY, 1976.

(24) Hoffman, J. D.; Miller R. L.; Marand H.; Roitman, D. B. Macromolecules 1992, 25, 2221.

(25) Lauritzen, J. I. *J. Appl. Phys.* **1973,** *44*, 4353.

(26) Sanchez, I. C.; DiMarzio, E. A. *J. Chem. Phys.* **1971**, *55*, 893.

(27) Armistead, J. P.: Hoffman, J. D. *Macromolecules* **2002**, *10*, 3895.

(28) Phillips, P. J.; Vatansever, N. *Macromolecules* **1987**, *20*, 2138.

(29) Monasse, B.; Haudin, J. M. *Makromolek. Chem. Macromolek. Symp.* **1988**, *20-1*, 295.

(30) Larcano, S.; Fatou, J. G.; Marco, C.; Bello, A. *An. Fis*. **1988**, *B-84*, 197.

(31) Larcano, S.; Fatou, J. G.; Marco, C.; Bello, A. *Eur. Polym. J*. **1989**, *25*, 1213.

(32) Vasanthakuman, R.; Pennis, A. J. *Polymer* **1983**, *24*, 175.

(33) Mazzullo, S.; Paganetto, G.; Celli, A. *Progr. Colloid Polym. Sci.* **1992**, *87*, 32.

(34) Allen, R. C.; Mandelkern, L. *Polym. Bull.* **1987**, *17*, 473.

(35) Ding, N.; Amis, E. J. *Macromolecules* **1991**, *24*, 3906.

(36) Xu, J. N. Ph. D. dissertation, Virginia Polytechnic Institute and state University 1999.

(37) Alamo, R.; Fatou, J. G.; Guzmán, J. *Polymer* **1982**, *23*, 374.

(38) Allan, R. C. Ph. D. dissertation, School of Materials Engineering Science, Virginia Polytechnic Institute and State University **1981**.

(39) Clark, E. J.; Hoffman, J. D. *Macromolecules* **1984**, *17*, 878.

(40) Monasse, B.; Haudin, J. M. *Coll. Polym. Sci.* **1985**, *263*, 822.

(41) Xu, J.; Srinivas, S.; Marand, H.; Agarwal, P. *Maromolecules* **1998**, *31*, 8230.

(42) Rrodriguez-Arnold, J.; Bu, Z. Z.; Cheng, S. Z. D.; Hsieh, E. T.; Johnson, T. W.; Geerts, R. G.; Palackal, S. J.; Hawley, G. R.; Welch, M. B. *Polymer* **1994**, *35*, 5194.

(43) Pelzbauer, Z.; Galeski, A. *J. Polym. Sci.* **1972**, *C38*, 23.

(44) Lovinger, A. J.; Davis, D. D.; Padden Jr., F. J. *Polymer* **1985**, *26*, 1595.

(45) Barham, P. J.; Keller, A.; Otun, E. L.; Holmes, P. A. *J. Mater. Sci.* **1984**, *19*, 2781.

(46) Roitman, D. B.; Marand, H.; Miller, R. L.; Hoffman, J. D. *J. Phys. Chem.* **1989**, *93*. 6919.

(47) Chen, C. C.; Chen, M.; Tseng, I. M. *J. Macro. Sci. Part B. Phys.* **2002**, *B41*, 1043.

(48) Gan, Z. H.; Abe, H.; Doi, Y. *Biomacromolecules* **2000**, *1*, 704.

(49) Bassett, D. C.; Hodge, A. M.; Olley, R. H. *Proc. R. Soc. Lond.* **1981**, A377, 25.

(50) Muthukumar, M. *P. Natl. Acad. Sci. USA* **1999**, *96*, 11690.

(51) Sadler, D. M.; Gilmer, G. H. *Phys. Rev. Lett.* **1986**, *56*, 2708.

(52) Sadler, D. M. *Nature* **1987**, *326*, 174.

(53) Sadler, D. M.; Gilmer, G.H. *Phys. Rev. B* **1988**, *38*, 5684.

(54) Goldbeck-Wood, G. *Macromol. Symp.* **1994**, *81*, 221.

(55) Higgs, P. G.; Ungar, G. *J. Chem. Phys.* **1994**, *100*, 640.

(56) Sutton, S. J.; Vaughan, A. S.; Bassett, D. C. *Polymer* **1996**, *37*, 5735.

(57) Putra, E. G. R; Ungar, G. *Macromolecules* **2003**, *36*, 3812.

(58) Putra, E. G. R; Ungar, G. *Macromolecules* **2003**, *36*, 5214.

(59) Doye, J. P. K.; Frenkel, D. *Phys. Rev. Lett.* **1998**, *81*, 2160.

(60) Doye, J. P. K.; Frenkel, D. *J. Chem. Phys*. **1999**, *110*, 7073.

(61) Toda, A *J. Chem. Phys.* **2003**, *118,* 8446.

(62) Toda, A. *Polymer* **1991**, *32*, 771.

(63) Toda, A.; Keller, A. *Colloid Polym. Sci.* **1993**, *271*, 328.

(64) Miller, R. L.; Hoffman, J.D. *Polymer* **1991**, *32*, 963.

(65) Flory, P. J. *Trans. Faraday Soc.* **1955**, *51*, 848.

(66) Vanderhard, D. I.; Perez, E. *J. Polym. Sci. Polym. Phys. Ed.* **1987**, *25*, 1637.

(67) Laupretre, F.; Monnerie, L.; Barthelemy, I.; Vairon, J. P.; Sanzean, A.; Roussel, D. *Polym. Bull.* **1986**, *51*, 159.

(68) McFaddin, D. C.; Russell, K. E.; Kelusky, E. C. *Polymer* **1986***, 27*, 204.

(69) McFaddin, D. C. *Polymer* **1988**, *29*, 258.

(70) Perez, E.; Vanderhart, D. I.; Crist, B.; Howard, P. R. *Macromolecules* **1987**, *20*, 78.

(71) Perez, E.; Bello, A.; Perena, J. M.; Benavente, R.; Martinez, M. C.; Aguilar, C. *Polymer* **1989**, *30*, 1508.

(72) Alamo, R. G.; Vanderhart, D. L.; Nyden, M. R.; Mandelkern, L. *Macromolecules* **2000**, *33*, 6094.

(73) Kitamaru, R.; Nakaoki, T.; Alamo, R. G.; Mandelkern, L. *Macromolecules* **1996**, *29,* 6847.

(74) Vanderhart, D. I.; Perez, E. *Macromolecules* **1986**, *19*, 1902.

(75) Alamo, R. G.; Mandelkern, L. *Thermochimica Acta* **1994**, *238*, 155.

(76) Alamo, R. G.; Chan, E. K. M.; Mandelkern, L.; Voigt-Martin, I. G. *Macromolecules* **1992**, *25*, 6381.

(77) Alamo, R. G.; Viers, B. D.; Mandelkern, L. *Macromolecules* **1993**, ***26***, *5740*.

(78) Springer, H.; Hengse, A.; Hinrichsen, G. *J. Appl. Polym. Sci.* **1990**, *40*, 2173.

(79) Springer, H.; Hengse, A.; Hinrichsen, G. *J .Appl. Polym. Sci.* **1992**, *44*, 189.

(80) Kimura, K.; Shigemura, T.; Yuasa, S. *J. Appl. Polym. Sci.* **1984,** *29*, 3161.

(81) Wilfong, D. L.; Knight, G. W. *J. Polym. Sci. , Polym. Phys. Ed.* **1990**, *28*, 861.

(82) Sanchez, I. C.; Eby, R. K. *Macromolecules* **1975**, *8*, 638.